ADVANCED MATERIALS
www.advmat.de

Solving Efficiency–Stability Tradeoff in Top-Emitting Organic Light-Emitting Devices by Employing Periodically Corrugated Metallic Cathode

Yu Jin, Jing Feng, Xu-Lin Zhang, Yan-Gang Bi, Yu Bai, Lu Chen, Tian Lan, Yue-Feng Liu, Qi-Dai Chen, and Hong-Bo Sun**

Top-emitting organic light-emitting devices (TOLEDs) are attracting much attention since light outcoupling from the top allows the fabrication of OLEDs on opaque substrates.[1] It is particularly suitable for high-resolution and high information-content active matrix displays because of the higher aperture ratio and display image quality. The semi-transparent top cathode of a conventional TOLED is usually composed of multiple functional layers to achieve both optical transmission and effective electron injection.[2] An ultrathin layer of a reactive, low work function metal (~1 nm) is used for electron injection and a noble metal with high transparency is used to reduce the sheet resistance of the composite cathode and also as a protective layer for the underlying reactive metal and organic layers, for example, bi-layer cathodes of Al/Ag or Ca/Ag etc. Ag is a widely used protective layer because of its low optical absorption and high conductivity. The Ag layer should be less than 20 nm to ensure a high transparency, however, more pinholes are formed in the Ag film because of poor film continuity for such a thin film, which results in easy diffusion of water and oxygen from air into the devices and accelerates the degradation of the devices.[3,4] Thicker Ag layers offer higher film continuity, however, the higher device stability comes at the expense of lower efficiency because of the decreased optical transmittance. Obviously, there exists a fundamental tradeoff between device stability and efficiency in conventional TOLEDs, which is really a challenge for their further applications.

Employing a periodic corrugation in the metal cathode of the TOLEDs provides a possibility to optimally solve the tradeoff. It is well known that surface-plasmon polaritons (SPPs) can be optically excited by incident radiation if the metal surface in which the SPPs reside shows a periodic corrugation to satisfy conversion of energy and momentum.[5–8] SPP-mediated emission from an OLED incorporating a periodic wavelength scale microstructure has been observed.[9–11] In the case of a thin metal film, SPP excitation on the opposite interface can be supported, and they can couple to each other by the familiar grating-coupling mechanism.[12,13] This results in a much enhanced light transmission through the classically opaque metal film,[14–16] and permits a relatively thick metal film of ~50 nm,[17] which is much more effective in protecting the devices from exposure to atmosphere. In the case of the TOLEDs, the reflective anode and semitransparent cathode are parallel to each other and form a microcavity. The cavity length is fixed by the distance between the two parallel electrodes and defines its resonant wavelength. In this case, the cross coupling occurs between the SPP modes associated with the top surface of the cathode and the microcavity modes within the device, instead of the two SPPs, which also results in an enhanced light transmission. Taking into account that the SPP resonance can be tuned by adjusting the period of the corrugated metal film or the refractive index of the dielectric on the metal surface to coincide with the microcavity modes, the light transmission can be enhanced at a desired wavelength. Therefore, employing a periodically corrugated cathode opens a possible avenue to release the efficiency–stability tradeoff that persists in TOLEDs.

SPP-mediated light emission through metal films has been discussed by others, however, it has mainly focused on the enhanced photoluminescence.[18–20] Although the possibility of using SPPs to enhance the performance of electrical-pumped TOLEDs has been explored in previous works, the cross coupling between the SPPs and microcavity modes has not been thoroughly investigated and the improvement of the electroluminescence (EL) efficiency that could be achieved for TOLEDs by using a corrugated structure has not been examined quantitatively so far.[21–24] In this communication, we demonstrate that the introduction of a periodic corrugation into TOLEDs to realize a corrugated metal cathode is effective in relieving the tradeoff between device stability and efficiency, through the cross coupling of the SPPs associated with the Ag cathode surface and the microcavity modes within the TOLEDs. The thickness of the Ag cathode for the corrugated TOLEDs was increased from 20 to 45 nm, and both the device lifetime and efficiency are significantly improved, which has been examined by performing current density (*J*)–voltage (*V*)–luminance (*L*) and lifetime measurements of the electrically pumped TOLEDs.

The experimental realization of the proposed corrugated TOLEDs has been accomplished. **Figure 1**a schematically

Y. Jin, Dr. J. Feng, X.-L. Zhang, Y.-G. Bi, Y. Bai, L. Chen, T. Lan, Y. F. Liu, Dr. Q. D. Chen, Prof. H.-B. Sun
State Key Laboratory on Integrated Optoelectronics
College of Electronic Science and Engineering
Jilin University
2699 Qianjin Street, Changchun, 130012, P. R. China
E-mail: jingfeng@jlu.edu.cn; hbsun@jlu.edu.cn
Prof. H.-B. Sun
College of Physics
Jilin University
119 Jiefang Road, Changchun, 130023, P. R. China

DOI: 10.1002/adma.201103397

ADVANCED MATERIALS
www.advmat.de
www.MaterialsViews.com

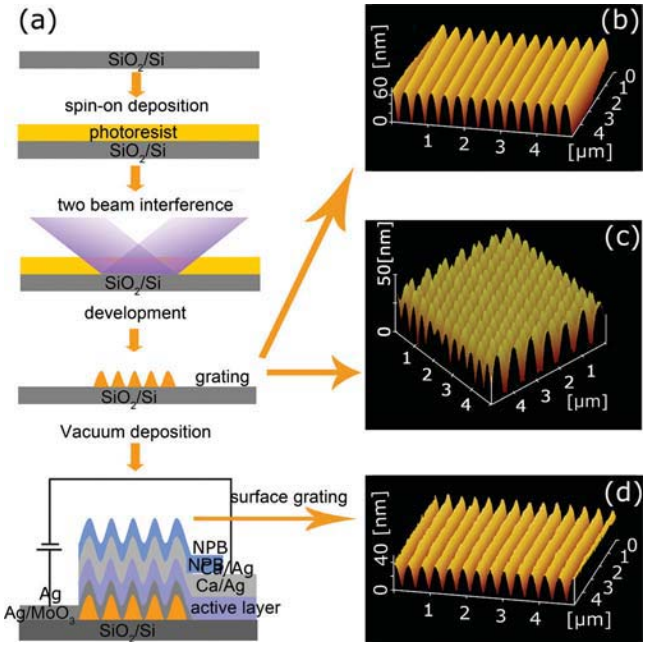

Figure 1. Scheme of introducing periodic corrugation into a TOLED by holographic lithography (a), and AFM images of the 1D (b) and 2D (c) grating on the photoresist surface and 1D grating on the Ag cathode surface (d).

illustrates the fabrication process, where the grating was introduced into the device by holographic lithography (Figure 1a). Both one-dimensional (1D) and two-dimensional (2D) gratings with a 350 nm period were fabricated on the surface of a photoresist film. The surface profile was investigated by atomic force microscopy (AFM), and the groove depth was determined to be around 60 and 50 nm for the 1D (Figures 1b) and 2D grating (Figure 1c), respectively, which is the optimized depth for the efficiency of the SPP coupling in OLEDs according to the results of previous works.[25] The following electrode and organic layers deposited by thermal evaporation duplicate the morphology of the photoresist, which is verified by the AFM measurements on the profile of the cathode surface (Figure 1d). The resonant wavelength of the microcavity as determined by the thickness of the organic layers between the two electrodes is around 600 nm, which coincides with the wavelength of the red dye employed in the devices. A capping layer was deposited onto the cathode surface to adjust the resonant wavelength of the SPPs at the Ag/capping layer interface by tuning its thickness to cross couple with the cavity modes in the TOLEDs. For comparison, conventional planar TOLEDs with an optimum thickness of the Ag cathode and capping layers are fabricated.

TOLEDs with different cathode thickness and with/without corrugation are designed to examine the effects of the cathode thickness as well as the corrugation on their EL performance. The schematic structures of six TOLEDs are shown in **Figure 2**, and their EL performances are compared in **Figure 3**. The luminance and current efficiency show significant differences for the six TOLEDs. There are two factors that govern the EL performance of the planar TOLEDs (devices A–D), i.e., the cathode thickness and the introduction of the capping layer. The light transmittance of the Ag layer is very sensitive to the layer thickness, and quickly decreased from 30% for 20 nm Ag to 5% for 45 nm Ag layers (inset in Figure 3c). Therefore the planar devices with a 20 nm Ag cathode and with/without a capping layer (device A and B) exhibit a higher EL performance than that of the devices with a 45 nm Ag cathode and with/without a capping layer (device C and D), respectively. The capping layer as a refractive index-matching layer shows an effect in improving the light transmittance in TOLEDs.[26] By comparing the four planar TOLEDs, device B with a capping layer and with a 20 nm Ag cathode shows optimum EL performance. However, in case of the corrugated TOLEDs (device E and F), both the luminance and current efficiency exhibit an obvious increment compared to the optimized planar devices, even though the cathode is increased to 45 nm. A photograph of the operating device is shown in the inset in Figure 3a. The central area with corrugation shows much brighter emission than that of the planar area. The current efficiency at the current density of 100 mA cm^{-2} is 7.1 and 7.4 cd A^{-1} for the 1D and 2D corrugated TOLEDs, respectively. This corresponds to a 22% and 28% enhancement compared to the optimized planar device (device B, 5.8 cd A^{-1} at 100 mA cm^{-2}), and 30% and 40% to the planar device with the thick cathode (device D, 5.3 cd A^{-1} at 100 mA cm^{-2}). In addition to the increased EL efficiency, an improved device stability is also expected, since the cathode thickness is increased to 45 nm, which is verified by the device lifetime measurement (Figure 3c). The half-luminance lifetime for the unencapsulated 1D corrugated TOLEDs is prolonged from 90 to 165 h at the initial luminance of 1000 cd m^{-2}, and from 24 to 70 h at the initial luminance of 10 000 cd m^{-2}, respectively. The above results indicate that the corrugated TOLEDs with thicker cathode layer exhibit not only

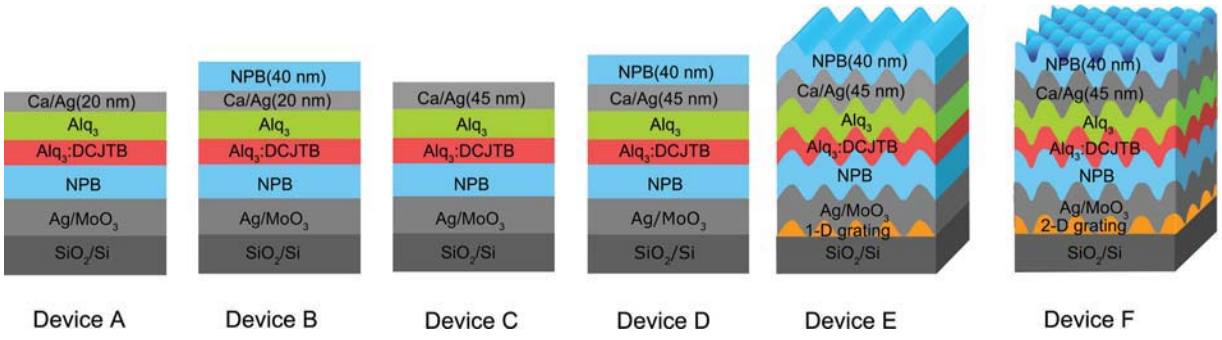

Figure 2. Schematic structures of TOLEDs with/without corrugation.

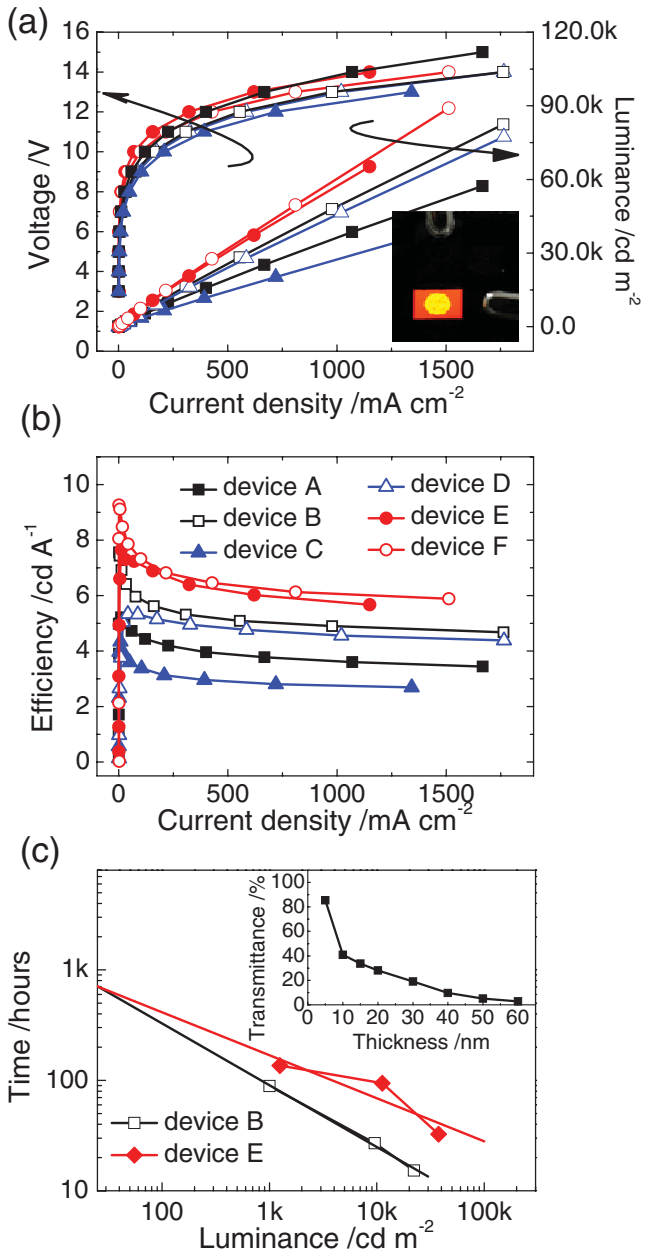

Figure 3. EL performance of the corrugated and planar TOLEDs. Current density–voltage–luminance (a), current density–efficiency (b) characteristics, and half-luminance lifetime of the device B and E (c), respectively. The inset in (a) shows a photograph of the operating corrugated and planar OLEDs at the same substrate and under same driving voltage. The inset in (c) shows the transmittance of the Ag film with varying thickness from 5 to 60 nm

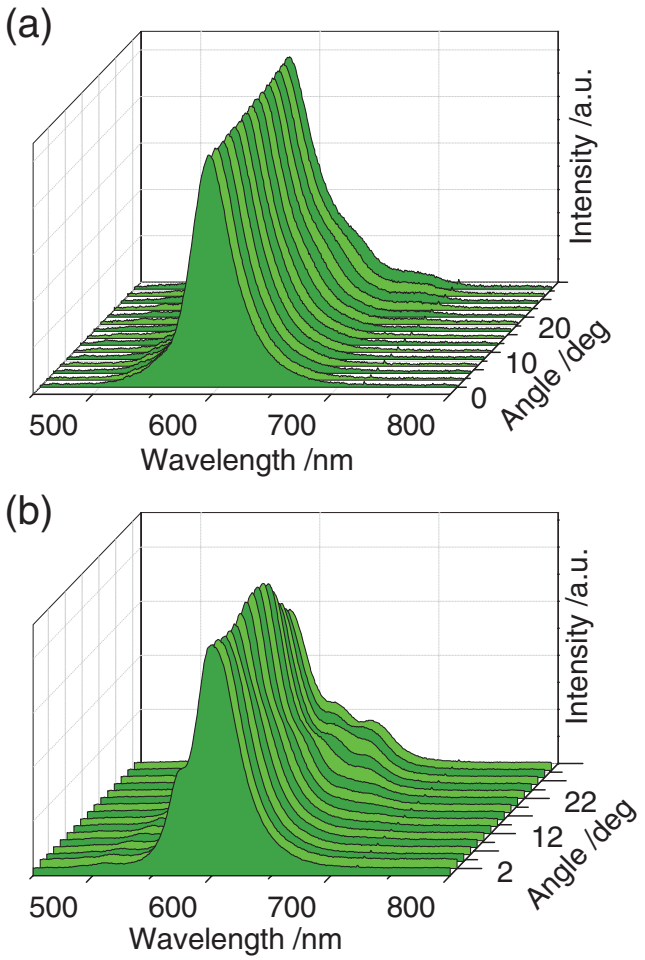

Figure 4. EL spectra at different observation angle from the corrugated TOLEDs with 1D (a) and 2D corrugation (b).

a higher EL efficiency but also a higher stability, which means that the persistent trade-off between them has been successfully released.

Understanding of the enhancement mechanism starts from analyzing the optical modes within the TOLEDs by measuring its emission spectra as a function of observation angle. **Figure 4** shows the EL spectra measured from the experimental devices employing 1D and 2D periodic corrugation at several observation angles off the surface normal. The optical modes appear as additional emission peaks in intensity which shift in wavelength as the angle varies, and have been observed in the EL spectra. To establish the optical modes supported by the microstructured TOLEDs, absorption spectra are simulated for the 1D periodic corrugation by employing a finite difference time domain (FDTD) method where the FDTD codes are in-house generated. The grating with a sinusoidal cross section and a fill factor of 50% was employed and the refractive index of the organic materials employed in the OLEDs was measured by ellipsometry for the simulation. The simulated dispersion map for the corrugated device and for transverse-magnetic (TM) polarization is shown in **Figure 5**a, in which the absorption intensity appears as a function of both incident angles and absorption wavelength. The dispersion relation curves constructed from the experimental EL emission spectra are also plotted. It can be seen that there is excellent agreement between the numerical calculation and experimental measurement. The optical modes within the device structure appear as EL maxima and indicate an efficient outcoupling of light from these optical modes by the addition of the appropriate wavelength-scale microstructure.

The observed optical modes for the corrugated devices have been identified by simulating the spatial magnetic field (H_y) distribution across the device structure as a function of position. Figures 5 b–d show the field distribution at the

ADVANCED MATERIALS
www.advmat.de

www.MaterialsViews.com

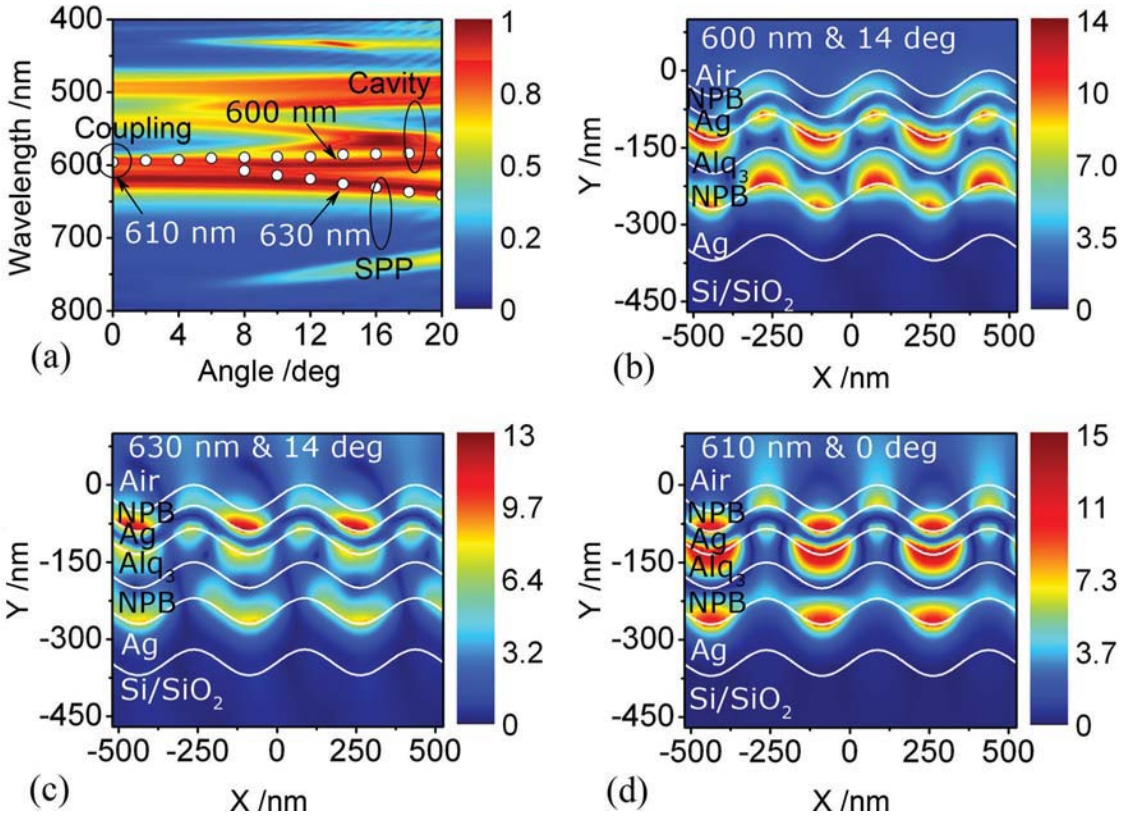

Figure 5. Calculated dispersion relation for the wavelength versus incident angle of the corrugated TOLEDs for TM polarization (a), and distribution of the magnetic field intensity in the corrugated TOLEDs at the wavelength of incident TM polarized light of 610 nm at 0° (b), 600 nm at 14° (c), and 630 nm at 14° (d), respectively. The measured dispersion relation extracted from the EL spectra (circles) is also shown in (a).

illumination wavelengths of 600, 630, and 610 nm in TM polarization, respectively, which correspond to the peak wavelengths of the measured EL emission at the observation angles of 14° and 0°, respectively. The field at the wavelength of 600 nm is mainly confined within the microcavity, which is assigned to the standing-wave microcavity mode (Figure 5b). The emission peak at 630 nm originates from SPP modes associated with the interface of the Ag cathode/capping layer, which decay exponentially into both media and reach a maximum at the interface (Figure 5c). The two modes meet at the wavelength of 610 nm and the normal direction, where the cross coupling occurs, which is clearly observed from Figure 5d. This cross coupling allows a mismatch in the in-plane wavevectors between the two modes to be overcome by the introduction to the metal cathode of a periodic microstructure, when the following condition is met,

$$k_{\mathrm{SPPorg/cap}} = k_{\mathrm{cavity}} \pm nk_{\mathrm{g}} \quad (1)$$

where n is an integer that describes the order of the scattering process, and $k_{\mathrm{SPPorg/cap}}$ *and* k_{cavity} are the in-plane wavevectors of the SPPs associated with the Ag cathode/capping layer interface and the microcavity modes within the TOLEDs, respectively. The coupling enables the transfer of energy across the metal cathode, and the SPPs may then scatter light, which contributes to the much enhanced light transmission.

The cross coupling that takes place at the peak wavelength of the emitting material employed in the TOLEDs (~600 nm) and at the normal direction is very crucial for the enhanced EL performance of the devices. In this work, the resonant wavelength corresponding to the microcavity modes is fixed at around 600 nm by the cavity length of the devices. The SPP resonant wavelength at the Ag cathode/capping layer has been adjusted to cross couple to the microcavity modes by tuning the thickness of the capping layer, so that its effective refractive index is tuned. The resonant wavelength of the SPP and the microcavity modes are far from each other at the normal direction and their cross couple occurs at large observation angles, when the capping layer is 100 nm (Figures S1 and S2, Supporting Information). With a reduction of the capping layer thickness, the SPP modes move close to the microcavity modes, and the angle for cross coupling is decreased. The cross couple is tuned to the normal direction at a 40 nm depth of the capping layer. Therefore, a much enhanced EL efficiency at the forward direction has been observed for the corrugated TOLEDs with a 40 nm capping layer and with the thicker Ag cathode. The TOLEDs employing a 2D microstructure show a higher EL performance compared to that of 1D corrugated TOLEDs, because of their greater efficiency in not only cross coupling between the SPP and the microcavity modes but the coupling of the SPPs to far-field radiation.[27]

In conclusion, the efficiency–stability tradeoff that existed in TOLEDs has been effectively released by employing a periodic microstructure in the device. The introduction of the periodic corrugation has allowed a much enhanced light transmission through a thick Ag cathode by the grating-induced cross coupling between the SPPs associated with the top interface of the cathode and the microcavity modes within the device cavity. An enhancement in both EL efficiency and device stability has been observed. Therefore, employing corrugation in the cathode of the TOLEDs is effective in overcoming the stability–efficiency bottleneck for their display and lighting applications.

Experimental Section

Preparation of Periodically Corrugated Substrate: A two beams laser interference microfabrication system was set up as shown in Figure 1a. A continuous laser with 266 nm wavelength (Coherent Inc.) was used as an irradiance light source. A layer of photoresist (150 nm, NOA-68, Norland Inc.) was spin-coated onto the cleaned SiO_2/Si substrate and exposed by two beams which were split from the UV laser with a beam size of ~6 mm in diameter. For fabrication of the 2D corrugation, the sample was exposed for a second time after rotation by 60°. After exposure, the sample was baked for 1 min (95 °C) and then developed in acetone. The morphologies of the microstructure were characterized by AFM (Digital Instruments Nanoscope IIIA) in the tapping mode.

OLED Fabrication and Evaluation: Prepared substrates coated with a corrugated photoresist film were immediately placed into a thermal evaporation chamber. A Ag anode (100 nm), a MoO_3 anodic modification layer (5 nm), a hole-transporting layer of *N*,*N*′-diphenyl-*N*,*N*′-bis 1,1′-biphenyl)-4,4′-diamine (NPB, 80 nm), an emitting layer (20 nm) of 0.8 wt% red dye (4-(dicyanomethylene)-2-t-butyl-6-(1, 1, 7, 7-tetramethyljulolidyl)-4*H*-pyran (DCJTB), doped tris-(8-hydroxyquinoline) aluminum (Alq_3), an electron-transporting layer of Alq_3 (45 nm), and a cathode of Ca (2 nm)/Ag (45 nm) were evaporated sequentially. Finally, a capping layer (40 nm) was deposited onto the cathode surface of the corrugated TOLEDs. For comparison, planar TOLEDs with a Ag cathode (20/45 nm) and with/without a capping layer were fabricated as controls. Here, all layers were prepared by thermal evaporation in a high vacuum (less than 5×10^{-4} Pa). The active area of the devices was 2 mm × 2 mm. Their current density–voltage–luminance (*J*–*V*–*L*) characteristics were measured by a Keithley 2400 programmable voltage–current source and a Photo Research PR-655 spectrophotometer. The emission spectra at different observation angles were measured by placing the TOLEDs on a rotating stage with one of the grooves parallel to the rotation axis. An aperture was used to limit the angular acceptance to ~1°. The *J*–*V*–*L* measurements were conducted in air at room temperature. The device lifetime measurements were conducted in a glove box without device encapsulation.

Supporting Information

Supporting Information is available from the Wiley Online Library or from the author.

Acknowledgements

The authors gratefully acknowledge support from 973 project (Grant Nos. 2011CB013005 and 2010CB327701) and NSFC (Grant Nos. 61177024, 60977025 and 90923037).

Received: September 3, 2011
Published online: January 25, 2012

[1] A. Dodabalapur, L. J. Rothberg, R. H. Jordan, T. M. Miller, R. E. Slusher, J. M. Phillips, *J. Appl. Phys.* **1996**, *80*, 6954.
[2] L. S. Hung, C. W. Tang, M. G. Mason, P. Raychaudhuri, J. Madathil, *Appl. Phys. Lett.* **2001**, *78*, 544.
[3] S. F. Lim, L. Ke, W. Wang, S. J. Chua, *Appl. Phys. Lett.* **2001**, *78*, 2116.
[4] D. Kolosov, D. S. English, V. Bulovic, P. F. Barbara, S. R. Forrest, M. E. Thompson, *J. Appl. Phys.* **2001**, *90*, 3242.
[5] W. L. Barnes, A. Dereux, T. W. Ebbesen, *Nature* **2003**, *424*, 824.
[6] W. C. Liu, D. P. Tsai, *Phys. Rev. B* **2002**, *65*, 155423.
[7] H. A. Atwater, A. Polman, *Nat. Mater.* **2010**, *9*, 205.
[8] T. Okamoto, F. H'Dhili, S. Kawata, *Appl. Phys. Lett.* **2004**, *85*, 3968.
[9] P. A. Hobson, S. Wedge, J. A. E. Wasey, I. Sage, W. L. Barnes, *Adv. Mater.* **2002**, *14*, 1393.
[10] C. J. Yates, I. D. W. Samuel, P. L. Burn, S. Wedge, W. L. Barnes, *Appl. Phys. Lett.* **2006**, *88*, 161105.
[11] J. M. Lupton, B. J. Matterson, I. D. W. Samuel, M. J. Jory, W. L. Barnes, *Appl. Phys. Lett.* **2000**, *77*, 161105.
[12] T. W. Ebbesen, H. J. Lezec, H. F. Ghaeml, T. Thio, P. A. Wolff, *Nature* **1998**, *391*, 667.
[13] I. R. Hooper, J. R. Sambles, *Phys. Rev. B* **2004**, *70*, 045421.
[14] R. W. Gruhlke, W. R. Holland, D. G. Hall, *Phys. Rev. Lett.* **1986**, *56*, 2838.
[15] S. Y. Nien, N. F. Chiu, Y. H. Ho, J. H. Lee, C. W. Lin, K. C. Wu, C. K. Lee, J. R. Lin, M. K. Wei, T. L. Chiu, *Appl. Phys. Lett.* **2009**, *94*, 103304.
[16] S. Wedge, W. L. Barnes, *Opt. Express* **2004**, *12*, 3673.
[17] S. Wedge, I. R. Hooper, I. Sage, W. L. Barnes, *Phys. Rev. B* **2004**, *69*, 245418.
[18] W. L. Barnes, W. A. Murray, J. Dintinger, E. Devaux, T. W. Ebbesen, *Phys. Rev. Lett.* **2003**, *92*, 107401.
[19] A. G. Brolo, S. C. Kwok, M. G. Moffitt, R. Gordon, J. Riordon, K. L. Kavanagh, *J. Am. Chem. Soc.* **2005**, *127*, 14936.
[20] S. Wdege, I. R. Hooper, I. Sage, W. L. Barnes, *Phys. Rev. B* **2004**, *69*, 245418.
[21] D. K. Gifford, D. G. Hall, *Appl. Phys. Lett.* **2002**, *81*, 4315.
[22] J. Feng, T. Okamoto, R. Naraoka, S. Kawata, *Appl. Phys. Lett.* **2008**, *93*, 051106.
[23] J. Feng, T. Okamoto, S. Kawata, *Appl. Phys. Lett.* **2005**, *87*, 241109.
[24] J. Feng, T. Okamoto, S. Kawata, *Opt. Lett.* **2005**, *30*, 2302.
[25] X. L. Zhang, J. Feng, J. F. Song, X. B. Li, H. B. Sun, *Opt. Lett.* **2011**, *36*, 3915.
[26] Q. Huang, K. Walzer, M. Pfeiffer, V. Lyssenko, G. He, K. Leo, *Appl. Phys. Lett.* **2006**, *88*, 113515.
[27] P. T. Worthing, W. L. Barnes, *Appl. Phys. Lett.* **2001**, *79*, 3035.